Electrospun TiO_2 Nanorods with Carbon Nanotubes for Efficient Electron Collection in Dye-Sensitized Solar Cells

*Lijun Yang and Wallace Woon-Fong Leung**

A dye-sensitized solar cell (DSSC) based on mesoporous TiO_2 is a promising low-cost, high-efficiency photovoltaic device for solar energy conversion.[1–3] To date, a power conversion efficiency (PCE) of 12.3% has been obtained. Despite this, further improvement is necessary for DSSCs to compete with the performance of silicon-based solar cells.[4]

In a conventional DSSC, a monolayer of molecular dye is adsorbed at the surface of a mesoporous wide bandgap semiconductor oxide film, such as TiO_2 or ZnO. However, electron transport in nanoparticle-based devices is limited by a trap-limited diffusion process. The slow charge diffusion increases the probability of recombination, resulting in a lower efficiency. Moreover, the grain boundaries encountered during electron transport lead to fast recombination prior to their collection at the electrode. Much effort has been devoted to improve charge transport properties and collection efficiency.

One promising solution is to use a one-dimensional (1D) nanostructure photoanode to replace the nanoparticle film, which provides a direct pathway for collection of charges generated throughout the device. Electron transport in 1D nanostructures, such as nanowires, nanofibers, and nanorods, is expected to be several orders of magnitude faster than that of nanoparticles.[5–8] Another approach to improve the electron transport and collection is by incorporating highly electrically conductive materials, such as carbon tubes and graphite, in titanium photoanode. The presence of conductive materials in an titanium photoanode is expected to improve the charge transport properties and extend the electron lifetime, thereby improving the performance of the device. Several groups have reported that utilizing nanocomposite photoanodes, such as titanium/carbon nanotubes and titanium/graphene, can enhance electron transport and collection efficiency.[9–12]

Based on the idea of deploying a direct-charge transport superhighway, 1D nanomaterials, TiO_2 nanorods, and multiwalled carbon nanotubes were incorporated into a photoanode for a DSSC. Specifically, the multiwall carbon nanotubes (MWCNTs) are inserted in the TiO_2 nanorod by electrospinning with a simple one-step approach. Incorporating the MWCNT into the TiO_2 nanorod can enhance the charge transport rate and improve the efficiency of the device. A high efficiency of 10.24% has been achieved with a high fill factor (FF) of 74%.

Incorporating CNT into a titanium nanosphere photoanode has been reported in the literature.[13–15] However, we have included one important step, that is to replace the previous attempt of using a nanosphere by the 1D titanium nanostructure to further improve the charge transport properties. In our architecture, CNTs are inserted inside the TiO_2 nanorods. The electron transport routes in these three different architectures are depicted in **Scheme 1**. When comparing all three routes, electrons should be most effectively transported and collected in Scheme 1c, minimizing electron loss.

Figure 1a displays the SEM image of TiO_2 nanorods incorporating MWCNTs. The diameter of the nanorod is approximately 70 nm, and the length of the nanorods is of the order of hundreds of nanometers. Note that the MWCNT is not visible from the SEM image, which suggests that the MWCNT might be in the TiO_2 nanorods. Figure 1b–d display the related TEM images. From the TEM image of the MWCNTs (Figure 1b), it can be seen that the outside diameter of the MWCNT ranges from 7 to 12 nm and the inside diameter is about 3 nm. The electrospun TiO_2 nanorods that incorporate the MWCNTs exhibit clear crystal lattice fringes (Figure 1c and d). The crystal inter-planar spacing of the TiO_2 grains is about 0.35 nm, which corresponds to the (101) planes of the anatase phase. On the other hand, the crystal inter-planar spacing of 0.34 nm corresponds to the (002) plane of the MWCNT. The foregoing morphology analysis indeed confirmed that the MWCNTs were inside the TiO_2 nanorods.

XPS spectra of the TiO_2 nanorod photoanode with and without MWCNTs were measured (**Figure 2**) to further confirm the presence of CNTs in the TiO_2 nanorods. The results show that the C 1s peak of the photoanode with 0.1 wt% MWCNTs (in precursor solution for electrospinning) was stronger than that without, which suggests that the MWCNTs were successfully incorporated in the TiO_2 nanorods of the photoanode.

The Raman spectra of MWCNTs, and electrospun TiO_2 without and with MWCNTs, can be seen in Figure S1. For the disorder-induced D-band and G-band modes of MWCNTs, peaks that correspond to 1375 and 1575 cm^{-1} were observed; the D/G band ratio was 0.93. It is interesting to observe that the intensity of G-band modes of MWCNTs was reduced when the MWCNTs were incorporated in the TiO_2 nanorods, while a new peak was observed at a lower frequency of approximately at 1850 cm^{-1}, which corresponds to the 1D linear C-chains that consist of more than 40 atoms inside the MWCNTs.[16,17]

To investigate the effect of the thickness of the photoanode on the performance of the DSSC device, two sets of devices each with different photoanode thickness, 6.6 ± 0.7 μm and 14.3 ± 0.3 μm, respectively, have been developed for testing. Furthermore, for each device the effect of different MWCNT concentrations in precursor solutions (0.05, 0.10, and 0.15%, respectively) on the performance of the device was studied as well. The performance of devices with TiO_2 nanofiber

L. Yang, Prof. W. W.-F. Leung
Department of Mechanical Engineering
The Hong Kong Polytechnic University
Hung Hom, Kowloon, Hong Kong, HKSAR
E-mail: mmwleung@polyu.edu.hk

DOI: 10.1002/adma.201204256

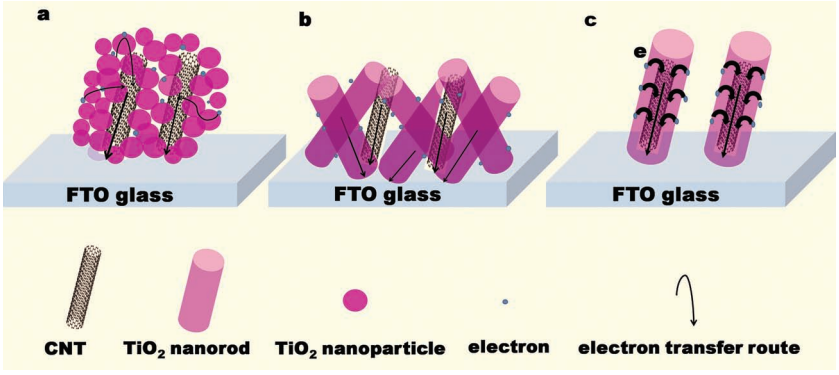

Scheme 1. Electron transport across photoanode: (a) CNTs totally surrounded/embraced by TiO_2 nanoparticles, (b) CNTs totally surrounded/embraced by TiO_2 nanorods, and (c) CNTs inside TiO_2 nanorods. The thickness of the arrow represents the electron transport speed, with thicker arrow representing faster electron transport.

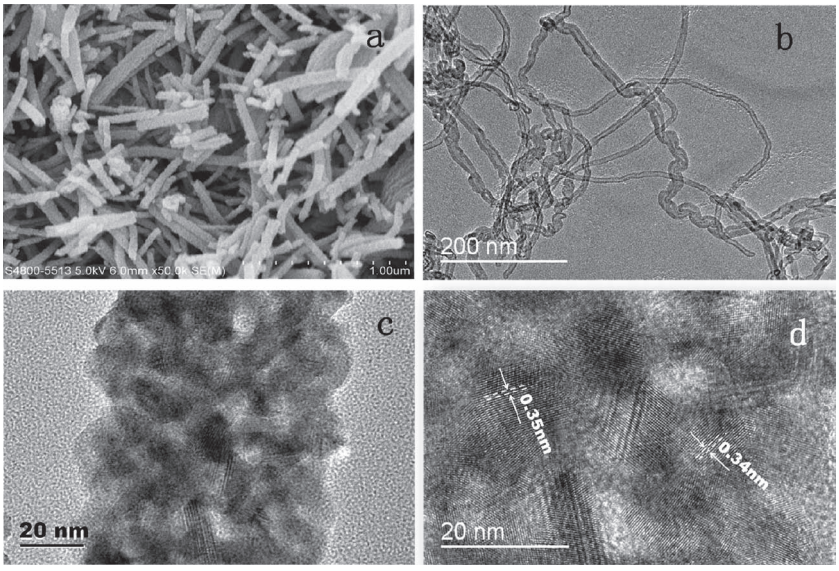

Figure 1. SEM and TEM images: a) SEM image of TiO_2 nanorods incorporating MWCNTs; b) and c) are TEM images, respectively, of MWCNTs and TiO_2 nanorods incorporating MWCNTs. d) HRTEM image of TiO_2 nanorods that incorporate MWCNTs.

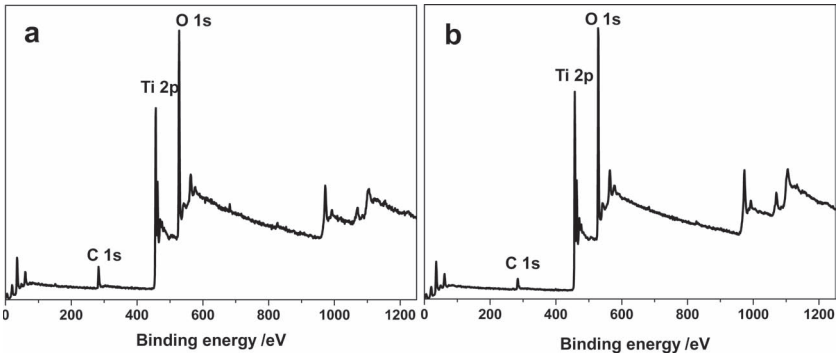

Figure 2. XPS spectra of photoanode: a) with MWCNTs (0.1 wt% in precursor solution), and b) without MWCNTs.

photoanodes without the incorporation of MWCNTs served as reference.[6] **Figure 3** shows the typical photocurrent–voltage (J–V) performance curves of these devices. The details of the photovoltaic parameters were listed in **Table 1**. From the J–V curves, it can be seen that the fill factor (FF) has been improved through introducing the MWCNT in the photoanode. With the same amount of MWCNT, the thicker photoanode shows both higher short-circuit current density (J_{sc}) and open-circuit voltage (V_{oc}). It is worth to note that the photoanode with thickness of 14.3 ± 0.3 μm was the optimized thickness, which can be seen in Table S1. To investigate the effect of the dosage of MWCNT in the photoanode on the performance of the device, different samples with weight percentages of MWCNT from 0.05% to 0.15% in the precursor solution for electrospinning were prepared. **Figure 4** shows the effect of amount of MWCNT on both J_{sc} and FF. By increasing the concentration of MWCNT from 0.05% to 0.1% for the thinner photoanode, J_{sc} improved from 8.92 to 11.1 $mAcm^{-2}$, which represents a 24% increase. Similar approach shows that 30% enhancement can be realized for the thicker photoanode. However, upon further increase in the amount of MWCNT to 0.15%, J_{sc} decreased in both sets of photoanode devices. Despite this reverse trend, the FF kept increasing with increasing the amount of MWCNT. Measurement of the external quantum efficiency (EQE) was carried out to further investigate the mechanism of enhancement in device performance. As seen in **Figure 5**, the normalized EQE response at all wavelengths is enhanced when the concentration of MWCNT in the precursor solution was increased from 0.05% to 0.10%. However, further increase in the concentration of MWCNT to 0.15%, results in reduction in EQE at all wavelengths. This can be understood from the following. Given the MWCNT is incorporated inside the photoanode, this can rapidly capture and transport the photogenerated electrons and concurrently reduce the undesirable recombination and back-reaction. Therefore, at low MWCNT concentration increasing the amount of MWCNT in the photoanode improves the charge collection efficiency and reduces the recombination, which results in improved performance (J_{sc}, EQE). However, at higher concentration of MWCNT, there is competition on light harvesting between dye molecules (N719) and MWCNT, and as a result the dye loading capacity and thus the efficiency are both reduced.[10] There could be

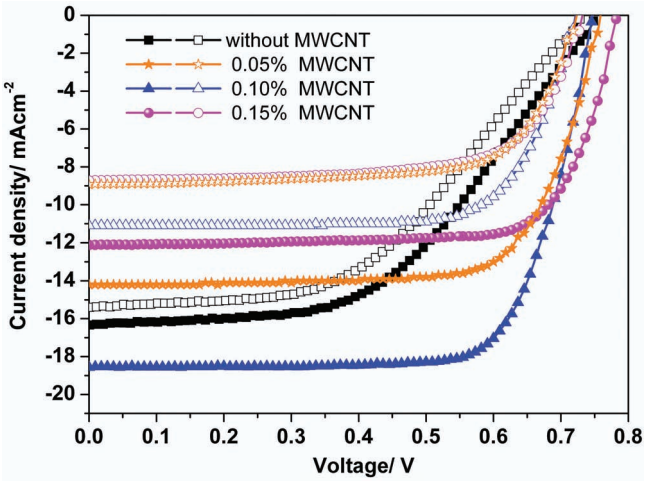

Figure 3. *J–V* characteristics of different photoanodes, hollow-symbol curve represents thinner photoanode with thickness about 6.6 ± 0.7 μm, and solid-symbol curve represents thicker photoanode with thickness about 14.3 ± 0.3 μm.

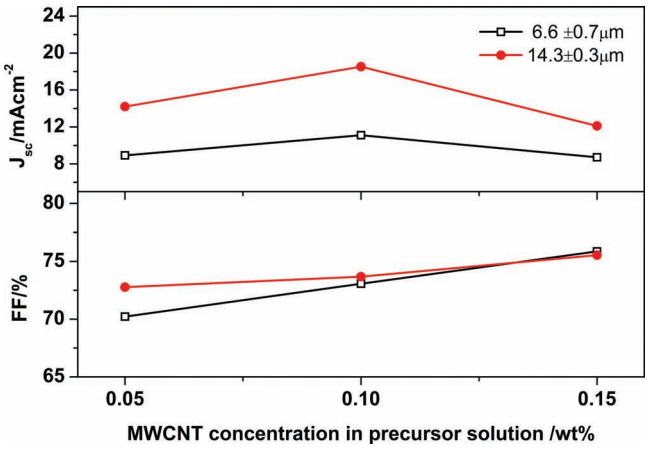

Figure 4. The effect of MWCNT concentration in the precursor solution on J_{sc} and FF.

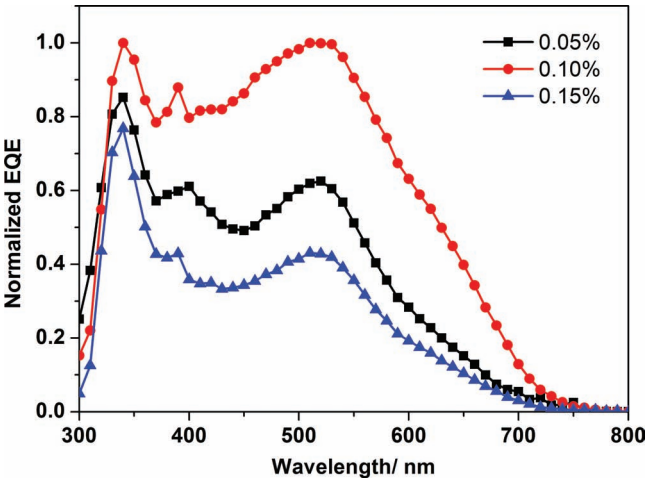

Figure 5. Normalized EQE spectra of a thicker photoanode with different MWCNT concentration in the precursor solution.

other more complicated mechanisms involved with MWCNT overdose. Therefore, it is necessary to optimize the amount of MWCNTs in the photoanode to balance the electron transport properties and dye loading capacity. Upon optimization of the parameters for the photoanode, a high efficiency of 10.24% has been attained for a photoanode with nanorods that incorporates 0.1% MWCNTs in the precursor solution. It is worthy to note that the improved efficiency for the photoanode incorporating MWCNTs is largely due to the improved FF. Based on our previous studies,[6] the FF of devices without incorporating MWCNTs in the photoanode was typically between 50 and 55%. By incorporating MWCNT in the photoanode, the FF is boosted to 70–75%, which is a 35% increase. Therefore, introducing MWCNTs in a photoanode can improve the charge transport properties and suppress recombination, both of which lead to an improvement of the charge collection efficiency.

In summary, MWCNTs, which perform as an ideal electron transport superhighway, are introduced inside TiO_2 nanorods. This configuration is successfully applied in a photoanode to improve the performance of a DSSC device. Different concentrations of MWCNTs in a precursor solution for electrospinning on the device performance have been investigated. The FF of the DSSC device increases as the MWCNT amount in the nanorods increases from 0.05% to 0.15% (in precursor solution). The J_{sc} first increases due to improved electron charge transport and

Table 1. Photovoltaic parameters for DSSC with different photoanode.

MWCNTs in wt% in precursor solution	Thickness [μm]	V_{oc} [V]	J_{sc} [mAcm^{-2}]	FF [%]	PCE [%]
0[6]	7.90	0.73	15.40	50.08	5.63
	16.7	0.74	16.30	51.24	6.18
0.05%	6.70	0.72	8.92	70.22	4.51
	14.47	0.76	14.20	72.27	7.80
0.10%	6.04	0.72	11.10	73.07	5.84
	14.64	0.75	18.53	73.68	10.24
0.15%	7.32	0.73	8.72	75.87	4.38
	13.97	0.78	12.11	75.54	7.13

subsequently it decreases due to a lower dye loading capacity of the photoanode at high MWCNT concentration. At a 0.1% MWCNT concentration, the DSSC device exhibits the highest efficiency of 10.24%, with a high J_{sc} of 18.53 mA cm^{-2} and a FF of 74%. The improved efficiency is largely due to the improved FF. These positive results confirm that the electrospun nanorods that incorporate CNTs provide an effective means to utilize economical materials optimally for developing a photoanode with efficient charge transport properties for realizing solar energy conversion in the future.

Experimental Section

TiO_2/PVP/MWCNT composite nanofibers were first electrospun on fluorine-doped tin oxide (FTO) glass (15 Ω per square) from a precursor solution that contained titanium isopropoxide (TIP, 4 g), polyvinylpyrrolidone (PVP, 3.5 g), acetic acid (2 g), MWCNT(0.05–0.15 g), and ethanol(100 mL). All materials were obtained from Sigma-Aldrich and used without further purification. The voltage of 70 kV was applied over a collector distance of 19 cm. A layer of TiO_2/MWCNT nanorod were peeled off from the original FTO glass after calcination and then transferred to another FTO glass with an ultra-thin adhesive TiO_2 paste. The TiO_2/MWCNT nanorod photoanode was obtained after calcinating at 450 °C for 2 h. The thickness of the photoanode was measured by a surface profiler (TENCOR P-10).

Before sensitization, the photoanode (3 mm × 3 mm) was first treated with an aqueous solution of $TiCl_4$ (40 mM) at 60 °C for 15 min. After treatment, the photoanode was washed with ethanol and dried in vacuum at 80 °C. Subsequently, it was immersed in a solution of 0.03 mM Ruthenium dye (N719) in absolute ethanol at 55 °C for 24 h. The soaked photoanode was then washed with ethanol to remove "unanchored" dye molecules and subsequently dried in vacuum at room temperature. Platinum-sputtered FTO glass was used as the counter electrode. The counter electrode and dye-anchored photoanode were assembled into a sandwich prototype with surlyn (DuPont, 25 μm). The internal space of the cell was filled with a liquid electrolyte, which consisted of 0.6 M 1-methy-3-propylimidazolium iodide (PMII), 0.05 M LiI, 0.05 M I_2, and 0.5 M 4-tert-butyl pyridine (TBP) in acetonitrile.

The photovoltaic characterization was carried out with a Keithley 2400 digital source meter under illumination at AM1.5G, 100 mW/cm^2 from a solar simulator ABET SUN 2000. The power density of the solar simulator was calibrated by a silicon reference cell (NIST) and monitored by a power meter throughout the testing. The external quantum efficiency (EQE) values were measured with an EQE system equipped with a xenon lamp (Oriel 66902, 300 W), a monochromator (Newport 66902), a Si detector (Oriel 76175_71580) and a dual channel power meter (Newport 2931_C).

Supporting Information

Supporting Information is available from the Wiley Online Library or from the author.

Acknowledgements

L.Y. thanks The Hong Kong Polytechnic University for support during her PhD studies.

Received: October 12, 2012
Published online: January 28, 2013

[1] M. Grätzel, *J. Photochem. Photobiol. C: Photochem. Rev.* **2003**, *4*, 145.
[2] B. O'Regan, M. Gratzel, *Nature* **1991**, *353*, 737.
[3] M. Law, L. E. Greene, J. C. Johnson, R. Saykally, P. Yang, *Nat. Mater.* **2005**, *4*, 455.
[4] A. Yella, H.-W. Lee, H. N. Tsao, C. Yi, A. K. Chandiran, M. K. Nazeeruddin, E. W.-G. Diau, C.-Y. Yeh, S. M. Zakeeruddin, M. Gratzel, *Science* **2011**, *334*, 629.
[5] S. H. Kang, S. H. Choi, M. S. Kang, J. Y. Kim, H. S. Kim, T. Hyeon, Y. E. Sung, *Adv. Mater.* **2008**, *20*, 54.
[6] L. Yang, W. W.-F. Leung, *Adv. Mater.* **2011**, *23*, 4559.
[7] O. K. Varghese, M. Paulose, C. A. Grimes, *Nat. Nanotechnol.* **2009**, *4*, 592.
[8] T. Krishnamoorthy, V. Thavasi, M. Subodh G, S. Ramakrishna, *Energy Environ. Sci.* **2011**, *4*, 2807.
[9] N. Yang, J. Zhai, D. Wang, Y. Chen, L. Jiang, *ACS Nano* **2010**, *4*, 887.
[10] K.-M. Lee, C.-W. Hu, H.-W. Chen, K.-C. Ho, *Sol. Energy Mater. Sol. Cells* **2008**, *92*, 1628.
[11] A. Kongkanand, R. Martínez Domínguez, P. V. Kamat, *Nano Lett.* **2007**, *7*, 676.
[12] X. Dang, H. Yi, M.-H. Ham, J. Qi, D. S. Yun, R. Ladewski, M. S. Strano, P. T. Hammond, A. M. Belcher, *Nat. Nanotechnol.* **2011**, *6*, 377.
[13] P. Brown, K. Takechi, P. V. Kamat, *J. Phys. Chem. C* **2008**, *112*, 4776.
[14] M. W. Marshall, S. Popa-Nita, J. G. Shapter, *Carbon* **2006**, *44*, 1137.
[15] S.-R. Jang, R. Vittal, K.-J. Kim, *Langmuir* **2004**, *20*, 9807.
[16] X. Zhao, Y. Ando, Y. Liu, M. Jinno, T. Suzuki, *Phys. Rev. Lett.* **2003**, *90*, 187401.
[17] V. Scuderi, S. Scalese, S. Bagiante, G. Compagnini, L. Durso, V. Privitera, *Carbon* **2009**, *47*, 2134.